Journal of Mechanics in Medicine and Biology
Vol. 22 (2022) 2250063 (24 pages)
© World Scientific Publishing Company
DOI: 10.1142/S0219519422500634

World Scientific
www.worldscientific.com

J. Mech. Med. Biol. Downloaded from www.worldscientific.com
by SWISS FEDERAL INSTITUTE OF TECHNOLOGY ZURICH (ETH) on 09/26/22. Re-use and distribution is strictly not permitted, except for Open Access articles.

BIO-MAGNETIC FLOW OF HEAT TRANSFER OVER MOVING HORIZONTAL PLATE BY THE PRESENCE OF VARIABLE VISCOSITY AND TEMPERATURE

SADIA ANJUM JUMANA*, M. FERDOWS*,‡ and E. E. TZIRTZILAKIS†

**Research Group of Fluid Flow Modeling and Simulation*
Department of Applied Mathematics
University of Dhaka, Dhaka 100, Bangladesh

†Fluid Mechanics and Turbomachinary Laboratory
Department of Mechanical Engineering
University of the Peloponnese, Tripoli, Greece
‡ferdows@du.ac.bd

Received 29 November 2021
Accepted 15 July 2022
Published 27 August 2022

This work aims at the investigation of 2D, steady, laminar, viscous, incompressible boundary layer and heat transfer flow of a biomagnetic fluid over a convectively heated moving horizontal plate in the presence of a magnetic dipole. It is assumed that the fluid viscosity is the inverse linear function of temperature and the temperature at the wall varies as power law function. The governing equations involve a system of coupled PDEs (momentum and energy equations) which are converted into a system of nonlinear ODEs by utilizing similarity transformations. The transformed ODEs along with the boundary conditions are then solved numerically by adopting a finite difference algorithm. The physical effects of the governing parameters (i.e., ferrohydrodynamic interaction parameter, buoyancy force parameter, viscosity-temperature parameter, wall parameter) on the flow fields along with the skin friction and heat transfer rate are presented. Verification of this work has been done by comparing former published results and acceptable agreement is found. It has been analyzed theoretically by using suitable transformations, that the ferrohydrodynamic interaction parameter, has a great enhancement effect on biomagnetic fluid rather than that on a regular fluid. It has been discovered that the inclusion of certain intensity of magnetic field along with the consideration of the variable viscosity and temperature, has significant effects on the flow and heat transfer mechanism. These outcomes could be of interest in medical as well as bioengineering implementations, like magnetic drug delivering in blood cells, separating RBCs (Red Blood Cells), controlling the flow of blood during surgeries and treating cancer by producing magnetic hyperthermia.

Keywords: Boundary layer; bio-magnetic fluid; heat transfer; finite difference method; variable viscosity; power-law variation.

‡ Corresponding author.

subito e.V. licensed customer copy supplied for Library and Information Service (SLI02X00670E)

J. Mech. Med. Biol. Downloaded from www.worldscientific.com
by SWISS FEDERAL INSTITUTE OF TECHNOLOGY ZURICH (ETH) on 09/26/22. Re-use and distribution is strictly not permitted, except for Open Access articles.

Nomenclature

Quantity	Symbol	Coherent SI unit
Buoyancy force parameter ($= \frac{\mathrm{Gr}_x}{\mathrm{Re}_x^2}$)	ξ	
Coordinate along the sheet	x	m
Coordinate normal to the sheet	y	m
Constant	a, A, γ	
Curie temperature	T_c	K
Density	ρ	$\mathrm{kg/m^3}$
Dimensionless stream function	f	
Dimensionless velocity	f'	
Dimensionless temperature	θ	
Dimensionless distance	α	
Dimensionless curie temperature	ϵ	
Dynamic viscosity	μ	kg/m s
Ferrohydrodynamic interaction parameter	B	T
Magnetization	M	A/m
Magnetic field intensity	H	A/m
Nusselt number	Nu	
Permeability	μ_0	$\mathrm{N/A^2}$
Prandtl number ($= \frac{\mu_\infty c_p}{\kappa}$)	Pr	
Reference temperature	T_r	K
Reference viscosity	μ_∞	kg/m s
Reynolds number ($= \frac{Ux}{\nu_\infty}$)	Re	
Shear stress	τ	$\mathrm{N/m^2}$
Similarity variable	η	
Skin friction factor	C_f	
Specific heat at constant pressure	c_p	J/kg·K
Stream function	ψ	$\mathrm{m^2/s}$
Temperature	T	K
Temperature at the fluid-sheet interface	T_w	K
Thermal conductivity	κ	W/m K
Velocity component along the sheet	u	m/s
Velocity component normal to the sheet	v	m/s
Velocity of the sheet	U	m/s
Viscosity-temperature parameter	θ_r	
Viscous dissipation parameter	λ	
Wall parameter	N	

1. Introduction

The inquiry of the ramification of magnetic field on fluids is important since there are numerous real-life appliances in a broad spectrum. The high-gradient magnetic

subito e.V. licensed customer copy supplied for Library and Information Service (SLI02X00670E)

J. Mech. Med. Biol. Downloaded from www.worldscientific.com
by SWISS FEDERAL INSTITUTE OF TECHNOLOGY ZURICH (ETH) on 09/26/22. Re-use and distribution is strictly not permitted, except for Open Access articles.

separation, targeted flow of drugs by magnetic particles as drug carriers, cell separation, treatment of cancer or tumor by magnetic hyperthermia, magnetic wound treatment, development of magnetic devices such as tracers are some of the practical applications, where magnetic field of various intensities are imposed. Numerous research works have been carried out on the reciprocation of the electromagnetic field with fluids such as in nuclear fusion, high-speed noiseless printing, cooling of transformer and medical science. Among the applications, the most overriding one is to find out the finest way in medical treatment and bioengineering. In medical application, hyperthermia is one of the treatments used for destroying cancer cells by exposing the body tissue to a slightly higher temperature. The mechanism of hyperthermia process is to implement magnetic field for increasing the temperature. Also, hyperthermia can be implemented for the eye lesion by the magnetic fluid application.

The biological fluids that prevail in living beings and whose flows are influenced by the appearance of magnetic fields, are defined as biomagnetic fluids. Since most of the biological fluids hold charged ions that associate with the exerted magnetic field, they are regarded as biomagnetic fluids. Especially blood is considered as the most significant biomagnetic fluid as the RBCs (red blood cells) present in blood embody hemoglobin particles, which are the ion-containing oxygen-transporting proteins. As a result, these hemoglobins, or the RBCs as a whole, can be influenced by the exerted magnetic fields. Furthermore, blood plasma is also affected by stronger steady magnetic fields due to its considerable concentration of flowing ions. Detailed effects of the magnetic field on the blood flow are published in Ref. 50.

Haik *et al.*[18] investigated the fluid dynamics of blood, one of the commonly used biomagnetic fluids, due to an applied magnetic field. The result of that investigation showed that the relation between the magnetic field and flow rate of biofluid, especially human bloods, is inversely proportional. That means, increment of magnetic field decreases the flow rate of human blood. An extention of Haik's initial biomagnetic fluid dynamic (BFD) model was developed by Tzirtzilakis.[50] According to this extended model, a biofluid is considered as laminar but not isothermal. The temperature distribution is studied in the flow field. According to the BFD model of the biofluid, flow along with an applied magnetic field is congruous with the governing rules of ferrohydrodynamics (FHD), Rosensweig[41,42] and the magnetohydrodynamics (MHD), Cramer,[14] Hughes,[20] Sutton[48] and Davidsson[15] where magnetization M plays the primary role. The magnetization is a function of the magnetic field intensity H and the temperature T for notifying the impacts of magnetic field on the bio-motion. The magnetization exerts a force which depends on the spatially varying magnetic field. Many studies have been conducted to explore the influence of magnetic field on human healthy pathological vessels.[27] Tzirtzilakis[51] examined the BFD flow in stenosis. Abi-Abdallah[1] studied the pulse magnetohydrodynamic blood motion in rigid vessels. The investigation of the MHD blood flow in stenosis assuming blood as non-Newtonian fluid with the help of Finite difference

subito e.V. licensed customer copy supplied for Library and Information Service (SLI02X00670E)

J. Mech. Med. Biol. Downloaded from www.worldscientific.com
by SWISS FEDERAL INSTITUTE OF TECHNOLOGY ZURICH (ETH) on 09/26/22. Re-use and distribution is strictly not permitted, except for Open Access articles.

method was done by Sankar.[45] The effect of magnetic field on blood flow through stenotic arteries has been discussed by Mamun.[26]

Misra[28] analyzed the biomagnetic fluid over a stretching sheet with the consideration of viscoelastic property of fluid. The impact of gravitational acceleration on unsteady biomagnetic fluid motion was investigated by Nor Amirah Idris.[37] Ferromagnetic liquid flow due to gravity aligned stretching sheet was studied by Rani Titus.[39] Various problem parameters such as, the temperature, skin friction and transfer rate of heat were found to be increasing in the presence of magnetic source. Mousavi[33] investigated numerically the influence of a nonuniform magnetic field on biomagnetic fluid flow in a duct with a constriction, where magnetic field was generated by a wire carrying electric current located outside the duct. The numerical simulation of biomagnetic micropolar blood flow considering the Rosensweig ferromagnetic formulation was carried out by Beg.[11] Ayeche[9] studied the two-dimensional time-dependent laminar hydromagnetic boundary-layer flow of a biomagnetic fluid over a wedge using a micropolar fluid model and taking into account the action of a transverse magnetic field.

The free-forced convective thin layer flow of incompressible fluid over a plate surface is another classical problem in fluid mechanics. Tzirtzilakis[49] presented the flow of heated ferrofluid passing through a stretching sheet which is not linear with externally applied magnetic field due to a magnetic dipole. This kind of flow of a biomagnetic fluid under the exertion of a confined magnetic field was investigated by Kafoussias.[22] Recently Muratza *et al.*[34] studied steady, two dimensional electrically-conducting blood over a stretching sheet. In that study they adopt both the principle of MHD and FHD and a numerical solution is obtained by employing an efficient numerical technique based on finite differences method. The effects of two inclined rectangular permanent magnetic field on heat transfer and flow characteristics of blood fluid in a channel, as a model of straight part of the aorta, have been investigated by Sharifi *et al.*,[8] using FHD principles. Considering the temperature at the stretching surface to follow a power law variation, and stretching velocity to have a nonlinear form with signum function or sign function, Murtaza *et al.*[31] described the biomagnetic flow and heat transfer. Moreover, the analysis of stability and convergence of an electrical conducting blood over a stretching sheet under the influence of a magnetic field was investigated by Murtaza *et al.*[34] where they found that the rate of heat transfer was enhanced and skin friction coefficient decreased with raising values of magnetic field. The duality solutions of biomagnetic fluid flow and heat transfer over a permeable quadratically stretching/shrinking sheet in the presence of a magnetic dipole was also investigated by the same author. Alam *et al.*[4] examined the influence of thermal radiation on biomagnetic fluid flow. The investigation of the biomagnetic flow along with heat transfer of an incompressible electrically conductive fluid (blood) containing various magnetic nanoparticles like ($CoFe_2O_4$, gold, Fe_3O_4,) over stretching surfaces in the presence of a magnetic dipole are carried out by Ferdows *et al.*[17,29] The inclusion of magnetic nanoparticle with blood flow has also been studied by Gul *et al.*[3] where they considered a computational model for

subito e.V. licensed customer copy supplied for Library and Information Service (SLI02X00670E)

J. Mech. Med. Biol. Downloaded from www.worldscientific.com
by SWISS FEDERAL INSTITUTE OF TECHNOLOGY ZURICH (ETH) on 09/26/22. Re-use and distribution is strictly not permitted, except for Open Access articles.

optimizing the magnetic navigation of MNs coated with the anticancer drugs inside the blood vessels.

Sakiadis[43] was the first mathematician who studied two-dimensional boundary-layer flow over a stretched surface moving with a constant velocity. Lately, Crane[13] extended Sakiadis[43,44] flow problem. Moreover, Crane's problem is one of the flow problems in the boundary-layer theory that possesses an exact solution. Karwe[23] studied the fluid flow and mixed convection transport from a moving plate in rolling and extrusion process. Later on, they found the numerical simulation of thermal transport associated with a continuously moving flat sheet in materials processing. Recently, the study of mixed convection flows or the combination of both free convection and forced convection have received a considerable attention from the researchers. Bachok *et al.*[10] studied a steady mixed convection of two-dimensional boundary-layer flow of an incompressible fluid through a moving vertical flat plate and they concluded that numerical solution depends on the value of the mixed convection parameter. They even found three solutions to the given problem. The effect of mixed convection on two-dimensional laminar flow over a continuously moving vertical surface considering suction or injection was studied by Ali.[5] A similar type of problem was studied by Ravindran,[40] with the additional terms of heat generation or absorption for unsteady case. Two-dimensional MHD boundary-layer flow in the presence of free convection over a moving sheet had been investigated by Singh[46] and they found that for buoyancy parameter, velocity profile and wall shear stress increases. The effects of variable viscosity and mixed convection on the flow and heat transfer on a continuously-moving stretching sheet was studied by Ali,[6] Pop[38] and Hassanien.[19] Steady thin-layer flow of a nanofluid over moving flat plate considering uniform free stream is reported by Najwa[35] through slip flow model. Thin layer flow of an MHD conducting fluid over impulsively started plate of infinite extent has been studied by Dholey.[16] Numerical investigation of flow and heat transfer of a fluid with a moving flat body with the cooperation of variable plate and streaming-free velocity is reported by Ferdows.[17]

Based on the above compositions, to the authors' knowledge, no prior research has been done on Bio-magnetic Blasius motion of heat transfer of fluid from a consistent plate over a moving surface due to suspended magnetic dipole while considering the variable viscosity and wall temperature variations. Similarity transformation with flow problem parameter and the effects of magnetic intensity on Blasius motion in the presence of ferrohydrodynamic principles are carried out. The principal equations are solved using Finite Difference scheme with a desired accuracy rate of 10^{-3} and then the numerical results of the flow profiles i.e., velocity profile and temperature profile have been presented graphically and discussed in the final section. Comparison tables are also included to verify the current work.

2. Mathematical Formulation of the Problem

The problem we consider here involves the 2D steady, laminar, mixed convective boundary-layer flow of a Newtonian viscous incompressible bio-magnetic fluid

subito e.V. licensed customer copy supplied for Library and Information Service (SLI02X00670E)

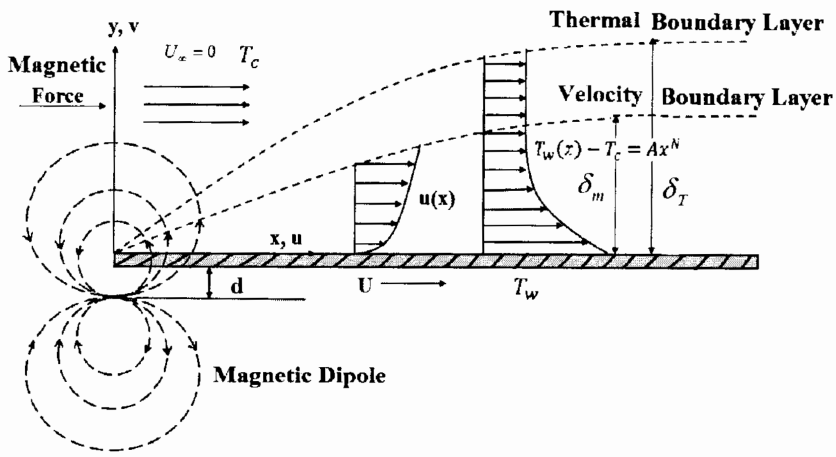

Fig. 1. Graphical illustration of the problem.

towards a continuously moving flat plate in the existence of a magnetic dipole situated at a distance d underneath the plate. The positive x-coordinate is measured along the moving surface and the positive y-coordinate is measured normal to the plate in the outward direction toward the fluid, as manifested in Fig. 1.The magnetic dipole generates a magnetic field of sufficient strength to infuse the fluid under consideration. The plate has been pondered to be at a fixed temperature $T_w < T_c$ and attains the temperature T_c far away from the plate. The temperature at the wall, T_w follows a power-law variation with the x-coordinate, defined by the relation $T_w(x) - T_c = Ax^N$. The plate moves continuously with a constant velocity U. The plate surface as well as the encompassing fluid are presumed to progress in the same direction.

Employing the boundary-layer approximation into account, the basic governing equations (continuity, momentum and thermal energy equations) can be written as, Kafoussias[22]:

$$\frac{\partial u}{\partial x} + \frac{\partial v}{\partial y} = 0, \tag{1}$$

$$u\frac{\partial u}{\partial x} + v\frac{\partial u}{\partial y} = \frac{1}{\rho_\infty}\frac{\partial}{\partial y}\left(\mu\frac{\partial u}{\partial y}\right) + g\beta(T - T_c) + \frac{\mu_0}{\rho_\infty}M\frac{\partial H}{\partial x}, \tag{2}$$

$$u\frac{\partial T}{\partial x} + v\frac{\partial T}{\partial y} + \frac{\mu_0}{\rho_\infty C_p}T\frac{\partial M}{\partial T}\left(u\frac{\partial H}{\partial x} + v\frac{\partial H}{\partial y}\right) = \frac{\kappa}{\rho_\infty C_p}\frac{\partial^2 T}{\partial y^2}. \tag{3}$$

Note that, the second term on the right side of the momentum Eq. (2) i.e., $g\beta(T - T_c)$ denotes the buoyancy force, whereas the third term i.e., $\frac{\mu_0}{\rho_\infty}M\frac{\partial H}{\partial x}$ denotes the magnetic body force per unit volume, and the third term on the left side of the thermal energy, Eq. (3), interprets the heating owing to adiabatic magnetization as in Andersson.[7] The ensuing boundary conditions are as follows:

$$\begin{aligned} &y = 0 : u = U, \quad v = 0, \quad T = T_w, \\ &y \to \infty : u \to 0, \quad T \to T_c. \end{aligned} \tag{4}$$

J. Mech. Med. Biol. Downloaded from www.worldscientific.com by SWISS FEDERAL INSTITUTE OF TECHNOLOGY ZURICH (ETH) on 09/26/22. Re-use and distribution is strictly not permitted, except for Open Access articles.

subito e.V. licensed customer copy supplied for Library and Information Service (SLI02X00670E)

J. Mech. Med. Biol. Downloaded from www.worldscientific.com
by SWISS FEDERAL INSTITUTE OF TECHNOLOGY ZURICH (ETH) on 09/26/22. Re-use and distribution is strictly not permitted, except for Open Access articles.

The variable-viscosity model assumes the viscosity of a viscous fluid to be an inverse proportional function of temperature.[25] Which is as follows:

$$\mu = \frac{\mu_\infty}{1 + \gamma(T - T_c)}. \tag{5}$$

Here, γ is a constant relating to thermal property and μ_∞ is the reference viscosity. By defining $a = \frac{\gamma}{\mu_\infty}$ and $T_r = T_c - \frac{1}{\gamma}$ Eq. (5) becomes

$$\frac{1}{\mu} = a(T - T_r). \tag{6}$$

Note that, $a > 0$ is incorporated with liquids whereas $a < 0$ with gases.[47] This is a better approximation for the flow since, with the application of the magnetic field, we seek even small disturbances of the temperature 1–3°C. These disturbances, even small, may be important during the application of the magnetic field and we include the variation of the viscosity with the temperature as well in order to increase the ability of prediction of the flow field near the area of the application of the magnetic field. Since we consider the variation of the magnetization with the temperature, we also include the variation of the viscosity with the temperature.

The magnetic scalar potential of the resulting magnetic field owing to the applied magnetic dipole is stated as[49]

$$V(x, y) = \frac{\alpha}{2\pi} \frac{x}{x^2 + (y + d)^2}. \tag{7}$$

The corresponding magnetic field $\vec{H}$ possesses the components

$$\begin{aligned} H_x &= -\frac{\partial V}{\partial x} = \frac{\alpha}{2\pi} \frac{x^2 - (y+d)^2}{[x^2 + (y+d)^2]^2}, \\ H_y &= -\frac{\partial V}{\partial y} = \frac{\alpha}{2\pi} \frac{2x(y+d)}{[x^2 + (y+d)^2]^2}. \end{aligned} \tag{8}$$

$\vec{H}$ can be written as

$$\vec{H} = \sqrt{H_x^2 + H_y^2} = \frac{\alpha}{2\pi} \left[\frac{1}{(y+d)^2} - \frac{x^2}{(y+d)^4} \right] \tag{9}$$

and the magnetic field components become

$$\begin{aligned} \frac{\partial H}{\partial x} &= -\frac{\alpha}{2\pi} \frac{2x}{(y+d)^4}, \\ \frac{\partial H}{\partial y} &= \frac{\alpha}{2\pi} \left[-\frac{2}{(y+d)^3} + \frac{4x^2}{(y+d)^5} \right], \end{aligned} \tag{10}$$

where $\alpha = \sqrt{\frac{U}{\nu_\infty x}} d$, represents dimentionless distance.

subito e.V. licensed customer copy supplied for Library and Information Service (SLI02X00670E)

J. Mech. Med. Biol. Downloaded from www.worldscientific.com
by SWISS FEDERAL INSTITUTE OF TECHNOLOGY ZURICH (ETH) on 09/26/22. Re-use and distribution is strictly not permitted, except for Open Access articles.

We assume that the applied $\vec{H}$ is strong enough to saturate the biomagnetic fluid and results in the magnetization M which varies linearly with temperature, Andersson[7] such that,

$$M = K^{*}(T_c - T), \tag{11}$$

where K^{*} is a constant called pyromagnetic coefficient.

In order to simplify the problem the subsequent dimensionless variables of transformation are introduced, Kafoussias,[22]

$$\begin{aligned} \eta(x,y) &= y\sqrt{\frac{U}{\nu_\infty x}}, \\ \psi(x,y) &= f(\eta)\sqrt{U\nu_\infty x}, \\ \theta(\eta) &= \frac{T - T_c}{T_w - T_c}. \end{aligned} \tag{12}$$

In terms of these dimensionless variables, the components of the velocity are obtained as

$$\begin{aligned} u &= \frac{\partial \psi}{\partial y} = Uf', \\ v &= -\frac{\partial \psi}{\partial x} = -\frac{1}{2}\frac{\nu_\infty}{x}\mathrm{Re}^{\frac{1}{2}}(f - \eta f'). \end{aligned} \tag{13}$$

Note that, implementing Eq. (5) in (12), the nondimensional temperature can be rewritten as

$$\theta(\eta) = \frac{T - T_r}{T_w - T_c} + \theta_r, \tag{14}$$

where $\theta_r = \frac{T_r - T_c}{T_w - T_c} = \frac{-1}{\gamma(T_w - T_c)}$. It is also noteable that $\theta_r > 0$ corresponds to gases and $\theta_r < 0$, to liquids.[47]

Applying the above relations, the dimensionless dynamic viscosity can now be derived as follows:

$$\begin{aligned} \mu &= \frac{\mu_\infty}{1 + \gamma(T - T_c)} = \frac{\mu_\infty}{1 + \gamma\left(T - T_r - \frac{1}{\gamma}\right)} = \frac{\mu_\infty}{1 + \gamma(T - T_r) - 1} = \frac{\mu_\infty}{\gamma(T - T_r)}, \\ &= \frac{\mu_\infty}{\gamma(T_c + \theta(T_w - T_c) - T_r)} = \frac{\mu_\infty}{\gamma(T_w - T_c)\left(\theta - \frac{T_r - T_c}{T_w - T_c}\right)} = \frac{-\mu_\infty \theta_r}{\left(\theta - \frac{T_r - T_c}{T_w - T_c}\right)}, \\ &= -\frac{\mu_\infty \theta_r}{(\theta - \theta_r)}. \end{aligned} \tag{15}$$

The continuity Eq. (1) is satisfied identically, whereas the momentum and energy Eqs. (2) and (3) get reduced to the ensuing nondimensional system of nonlinear ODEs as follows:

$$f''' - \frac{\theta'}{(\theta - \theta_r)}f'' - \frac{1}{2}\frac{(\theta - \theta_r)}{\theta_r}ff'' - \left(\xi + \frac{2B}{(\eta + \alpha)^4}\right)\frac{\theta(\theta - \theta_r)}{\theta_r} = 0, \tag{16}$$

subito e.V. licensed customer copy supplied for Library and Information Service (SLI02X00670E)

J. Mech. Med. Biol. Downloaded from www.worldscientific.com by SWISS FEDERAL INSTITUTE OF TECHNOLOGY ZURICH (ETH) on 09/26/22. Re-use and distribution is strictly not permitted, except for Open Access articles.

$$\theta'' + \frac{1}{2}\mathrm{Pr} f\theta' - N\mathrm{Pr} f'\theta - 2B\lambda(\theta+\epsilon)\left[\frac{f'}{(\eta+\alpha)^4} + \frac{(f-f'\eta)}{(\eta+\alpha)^5}\right] = 0. \tag{17}$$

The corresponding dimensionless boundary conditions emerge as

$$\begin{aligned} &f'(0) = 1, \quad f(0) = 0, \quad \theta(0) = 1, \\ &f'(\infty) = 0, \quad \theta(\infty) = 0. \end{aligned} \tag{18}$$

The dimensionless physical parameters, appeared in the transformed equations, are defined respectively as

$$\begin{aligned} \xi &= \frac{Gr_x}{\mathrm{Re}_x^2}, \quad \mathrm{Pr} = \frac{\mu_\infty C_p}{\kappa}, \\ \mathrm{Gr}_x &= \frac{g\beta(T_w - T_c)x^3}{\nu_\infty^2}, \quad \lambda = \frac{\mu_\infty U^2}{\kappa(T_w - T_c)}, \\ \mathrm{Re}_x &= \frac{Ux}{\nu_\infty}, \quad \epsilon = \frac{T_c}{(T_w - T_c)}, \\ B &= \frac{\alpha}{2\pi}\frac{K^*\mu_0(T_w - T_c)\rho_\infty}{\mu_\infty^2}. \end{aligned}$$

Skin friction factor, C_f and Nusselt number, Nu which are the main physical parameters of interest, are given by

$$C_f = \frac{2\tau_w}{\rho_\infty U^2} \quad \text{and} \quad Nu = \frac{q_w}{T_w - T_c}\frac{x}{k},$$

where $\tau_w = \mu \frac{\partial u}{\partial y}|_{y=0}$ and $q_w = -k\frac{\partial T}{\partial y}|_{y=0}$ are the shear stress and the flow rate at the plate, respectively.

Using Eq. (12) we can easily find τ_w and q_w and thus the nondimensional form of skin friction coefficient and the heat transfer rate becomes

$$C_f \mathrm{Re}^{1/2} = \frac{2\theta_r}{\theta_r - 1} f''(0), \tag{19}$$

$$\mathrm{Nu}/\mathrm{Re}^{1/2} = -\theta'(0). \tag{20}$$

3. Finite Difference Solution Technique

The transformed set of differential Eqs. (16) and (17) along with the corresponding boundary conditions (18) are solved by a simple yet efficient finite difference technique which is based on central differencing along with a tridiagonal matrix manipulation. It is basically an iterative algebraic solution procedure. In this procedure, the higher order DEs are first moderated into a set of second order DEs. These are then discretized with central spaced finite difference equations approximations. The nonlinear algebraic equations are subsequently linearized using Newton's method and the matrix–vector form is attained.

subito e.V. licensed customer copy supplied for Library and Information Service (SLI02X00670E)

J. Mech. Med. Biol. Downloaded from www.worldscientific.com by SWISS FEDERAL INSTITUTE OF TECHNOLOGY ZURICH (ETH) on 09/26/22. Re-use and distribution is strictly not permitted, except for Open Access articles.

The momentum Eq. (16) can be written as

$$f''' - \left(\frac{\theta'}{(\theta-\theta_r)} + \frac{1}{2}\frac{(\theta-\theta_r)}{\theta_r}f\right)f'' = \left(\xi + \frac{2B}{(\eta+\alpha)^4}\right)\frac{\theta(\theta-\theta_r)}{\theta_r}. \tag{21}$$

Now Eq. (21) can be contemplated as a second order DE by setting $y(x) = f'(\eta)$ provided that $f(\eta)$ and $\theta(\eta)$ are thought of as known functions. Then, Eq. (21) becomes

$$y''(x) - \left(\frac{\theta'}{(\theta-\theta_r)} + \frac{1}{2}\frac{(\theta-\theta_r)}{\theta_r}f\right)y'(x) = \left(\xi + \frac{2B}{(\eta+\alpha)^4}\right)\frac{\theta(\theta-\theta_r)}{\theta_r}. \tag{22}$$

Equation (22) can be written as,

$$M(x)y''(x) + L(x)y'(x) + O(x)y(x) = P(x), \tag{23}$$

where $M(x) = 1$, $L(x) = -(\frac{\theta'}{(\theta-\theta_r)} + \frac{1}{2}\frac{(\theta-\theta_r)}{\theta_r}f)$, $O(x) = 0$, $P(x) = (\xi + \frac{2B}{(\eta-\alpha)^4})\frac{\theta(\theta-\theta_r)}{\theta_r}$.

To start the solution procedure, we assume initial guesses for $f'(\eta)$ and $\theta(\eta)$ between $\eta = 0$ and $\eta = \eta_\infty(\eta \to \infty)$ which satisfy the boundary conditions (18). For this problem indicative initial guesses are as follows:

$$\begin{aligned} &f'(0) = 1 - \frac{\eta}{\eta_\infty}, \quad f(0) = \frac{\eta}{\eta_\infty}, \quad \theta(0) = 1 - \frac{\eta}{\eta_\infty}, \\ &f'(\infty) = 0, \quad \theta(\infty) = 0. \end{aligned} \tag{24}$$

The $f(\eta)$ distribution is obtained by integrating $f'(\eta)$. The next step is to consider $f(\eta)$ and $\theta(\eta)$ known and to determine a new estimation for $f'(\eta)$ i.e., $f'_{\text{new}}(\eta)$ by solving the nonlinear Eq. (21) using the above method. The distribution is updated by the integration of new $f'(\eta)$ curve. These new profiles of $f'(\eta)$ and $f(\eta)$ are then used for new inputs and so on. In this way, the momentum Eq. (16) is solved iteratively until convergence up to a small quantity ζ.

The energy Eq. (17) along with the boundary conditions (18) is solved by using the same algorithm. The Eq. (17) can be written as

$$\begin{aligned} &\theta'' + \frac{1}{2}\mathrm{Pr}f\theta' - \left(N\mathrm{Pr}f' + 2B\lambda\left[\frac{f'}{(\eta+\alpha)^4} + \frac{(f-f'\eta)}{(\eta+\alpha)^5}\right]\right)\theta \\ &\quad = 2B\lambda\epsilon\left[\frac{f'}{(\eta+\alpha)^4} + \frac{(f-\eta f')}{(\eta+\alpha)^5}\right]. \end{aligned} \tag{25}$$

By setting $y(x) = \theta(\eta)$ Eq. (25) becomes

$$\begin{aligned} &y''(x) + \frac{1}{2}\mathrm{Pr}fy'(x) - \left(N\mathrm{Pr}f' + 2B\lambda\left[\frac{f'}{(\eta+\alpha)^4} + \frac{(f-f'\eta)}{(\eta+\alpha)^5}\right]\right)y(x) \\ &\quad = 2B\lambda\epsilon\left[\frac{f'}{(\eta+\alpha)^4} + \frac{(f-\eta f')}{(\eta+\alpha)^5}\right]. \end{aligned} \tag{26}$$

Equation (26) can be written as

$$M(x)y''(x) + L(x)y'(x) + O(x)y(x) = P(x), \tag{27}$$

subito e.V. licensed customer copy supplied for Library and Information Service (SLI02X00670E)

J. Mech. Med. Biol. Downloaded from www.worldscientific.com by SWISS FEDERAL INSTITUTE OF TECHNOLOGY ZURICH (ETH) on 09/26/22. Re-use and distribution is strictly not permitted, except for Open Access articles.

where $M(x) = 1$, $L(x) = \frac{1}{2}\mathrm{Pr} f(\eta)$, $O(x) = -N\mathrm{Pr} f' - 2B\lambda[\frac{f'}{(\eta+\alpha)^4} + \frac{(f-f'\eta)}{(\eta+\alpha)^5}]$ and

$$P(x) = 2B\lambda\epsilon\left[\frac{f'}{(\eta+\alpha)^4} + \frac{(f-\eta f')}{(\eta+\alpha)^5}\right].$$

Considering $f(\eta)$ and $f'(\eta)$ known, we obtain new approximation $\theta_{\text{new}}(\eta)$ by solving Eq. (23) using the same method described earlier. This process continues until convergence up to ζ is attained.

This linear system is solved using the FORTRAN language with the help of Code-Blocks software. This is a free C, C++ and Fortran online environment created to permit fast computation of user-defined mathematical models. It is highly extensible and fully configurable and easy to program across multiple platforms. Although the FDM (Finite Difference Method) is an efficient yet simple numerical scheme, this method becomes unwieldy if complexities like unstructured domains or moving boundaries or mesh refinement or material discontinuities are required to be added in the problem.

By using trial and error method we set $\eta_\infty = 7$, step size, $\Delta\eta = 0.001$ and tolerance between iterations, $\zeta = 10^{-3}$ (the convergence criterion) in the finite difference code (FDC). Further, decrease in the step size barely manifests any significant changes in values. The choice of $\eta_\infty = 7$ ensures a sufficiently large infinity boundary condition and guarantees the convergence of every numerical solution to the asymptotic values precisely.

Verification

In order to verify our work, we have compared our results of the wall shear stress, (as for $-f''(0)$) and the Nusselt number ($-\theta'(0)$) for different values of Pr, N, θ_r with Soundalgeker[47] in Table 1. It is observed that the present outcomes approximate with the formerly found results quite well.

Table 1. Comparison of $-f''(0)$ and $-\theta'(0)$ for $\xi = 0$, $B = 0$ and various Pr, N, and θ_r.

			$-f''(0)$		$-\theta'(0)$	
Pr	N	θ_r	Present	Soundalgeker[47]	Present	Soundalgeker[47]
	0	−0.1	1.752	1.7399	1.121	1.1262
		−0.8	0.7981	0.7940	1.328	1.3288
		−2.0	0.6057	0.6029	1.361	1.3615
		−10.0	0.4802	0.4781	1.381	1.3816
		−15.0	0.4688	0.4668	1.383	1.3834
7	0.3	−0.1	1.841	1.8274	1.622	1.6283
		−0.8	0.8162	0.8121	1.859	1.8602
		−2.0	0.6121	0.6094	1.896	1.8969
		−10.0	0.4813	0.4792	1.919	1.9192
		−15.0	0.4695	0.4676	1.921	1.9212
	1	−0.1	2.013	1.9984	2.529	2.5346
		−0.8	0.8435	0.8394	2.795	2.7962
		−2.0	0.6214	0.6186	2.836	2.8367
		−10.0	0.4828	0.4808	2.860	2.8609
		−15.0	0.4706	0.4686	2.862	2.8630

subito e.V. licensed customer copy supplied for Library and Information Service (SLI02X00670E)

J. Mech. Med. Biol. Downloaded from www.worldscientific.com by SWISS FEDERAL INSTITUTE OF TECHNOLOGY ZURICH (ETH) on 09/26/22. Re-use and distribution is strictly not permitted, except for Open Access articles.

4. Computational Results and Discussion

This section provides the consequences of miscellaneous governing parameters on the flow as well as on the physical properties over the continuously moving sheet. The bio-magnetic fluid considered in this problem is human blood. For human body temperature $T = 310\,\text{K}$, the values of μ, c_p and κ are $3.2 \times 10^{-3}\,\text{kg/ms}$, $14.65\,\text{J/kgK}$ and $2.2 \times 10^{-3}\,\text{J/msK}$, respectively,[12] and hence $\Pr = 21$. The values of ϵ, λ and α are taken as -2, 1.6×10^{-3} and 1 respectively. Values of B are taken from 0 to 10,[49] and $B = 5$, where a fixed value is needed. For the variable wall parameter, N and viscosity-temperature parameter, θ_r we chose the values $(0, 0.3, 1)$ and $(-0.1, -0.5, -2, -10)$.[47] The buoyancy force parameter, ξ incorporates forced, mixed and free convection when $\xi \to 0 (\xi \ll 1)$, $\xi \sim 1$ and $\xi \gg 1$. So, we chose $(0.01, 1, 10)$ as the values of ξ.

In Figs. 2–5, we have shown the dimensionless velocity profiles for different values of B, N, θ_r and Pr along with different ξ, considering the fixed values $\Pr = 21$, $N = 0.3$, $\theta_r = -2.0$, $B = 5$, where needed. It is clear from all four figures that the buoyancy force parameter ξ has an increasing effect on the velocity profiles. As ξ increases from 0 to 10, the dimensionless velocity inside the boundary layer, increases from zero over the sheet to a certain value at the free stream representing an overshoot $(f(\eta) > 1)$ in the region $(0 \leq \eta \leq 1)$ and then converges to the boundary value. It is also noticed that near the leading edge of the sheet $(\xi \ll 1)$ forced convection is dominating, but as ξ increases $(\xi \sim 1)$, the flow moves into a mixed convection regime and subsequently into a free convection $(\xi \gg 1)$ dominated flow. It is interesting to note that, in Fig. 4, when the flow is dominated by free convection and the

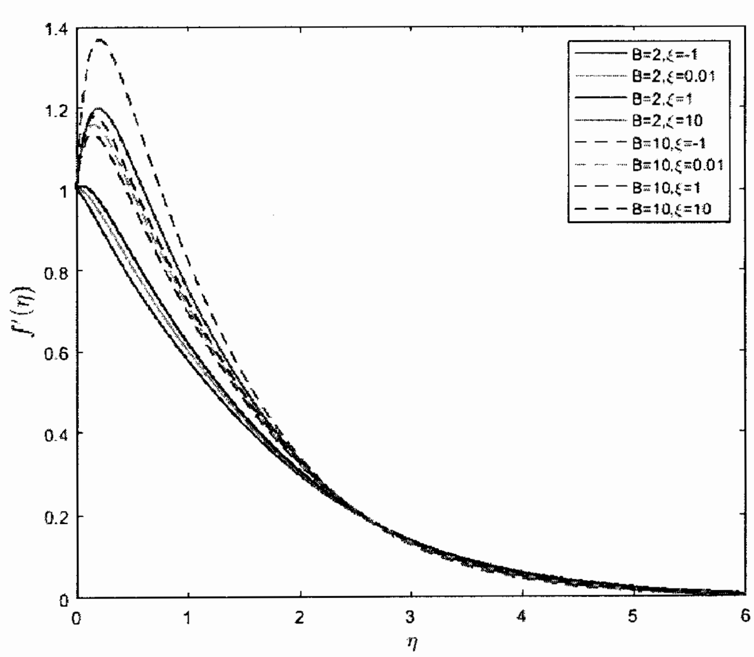

Fig. 2. $f'(\eta)$ versus η for different B and ξ.

subito e.V. licensed customer copy supplied for Library and Information Service (SLI02X00670E)

J. Mech. Med. Biol. Downloaded from www.worldscientific.com
by SWISS FEDERAL INSTITUTE OF TECHNOLOGY ZURICH (ETH) on 09/26/22. Re-use and distribution is strictly not permitted, except for Open Access articles.

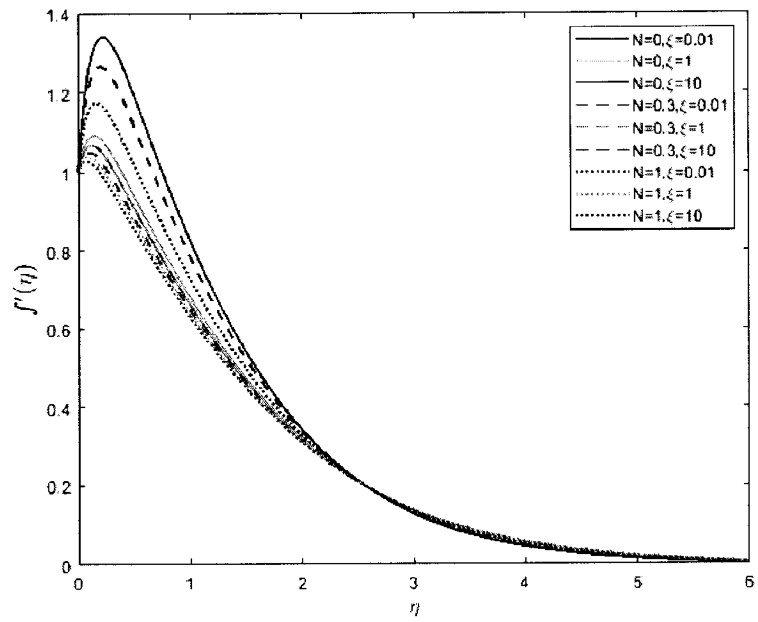

Fig. 3. $f'(\eta)$ versus η for different N and ξ.

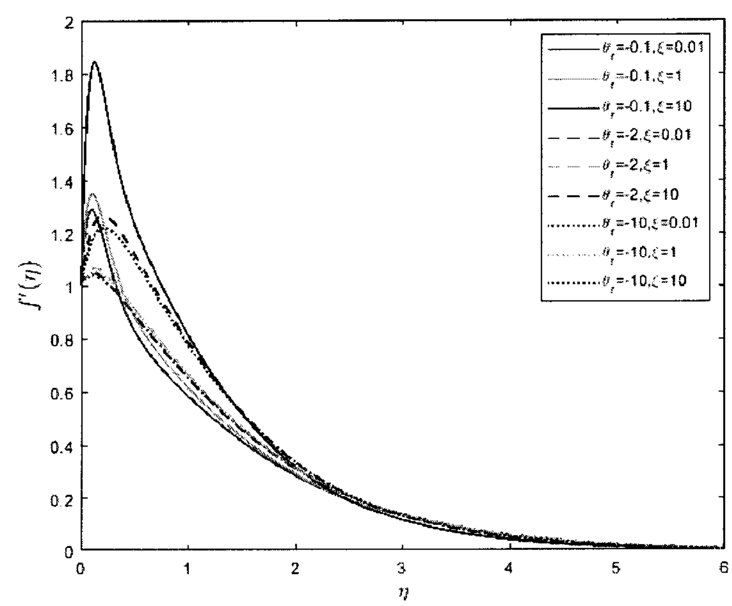

Fig. 4. $f'(\eta)$ versus η for different θ_r and ξ.

lowest viscosity-temperature parameter, $(\theta_r = -0.1)$, the flow obtains the highest velocity $(f'(\eta) \sim 1.8)$.

Whereas, for any fixed ξ, velocity profiles initially enhance with increasing B, and decreasing N, $|\theta_r|$ and Pr, respectively up to a separation point between $2 \leq \eta \leq 3$ $(\eta \sim 2.5)$ and after exceeding that point, the flow pattern is reversed. Also note that, higher values of B broaden the velocity boundary-layer thickness while higher values of N, $|\theta_r|$ and Pr narrow it down.

subito e.V. licensed customer copy supplied for Library and Information Service (SLI02X00670E)

J. Mech. Med. Biol. Downloaded from www.worldscientific.com
by SWISS FEDERAL INSTITUTE OF TECHNOLOGY ZURICH (ETH) on 09/26/22. Re-use and distribution is strictly not permitted, except for Open Access articles.

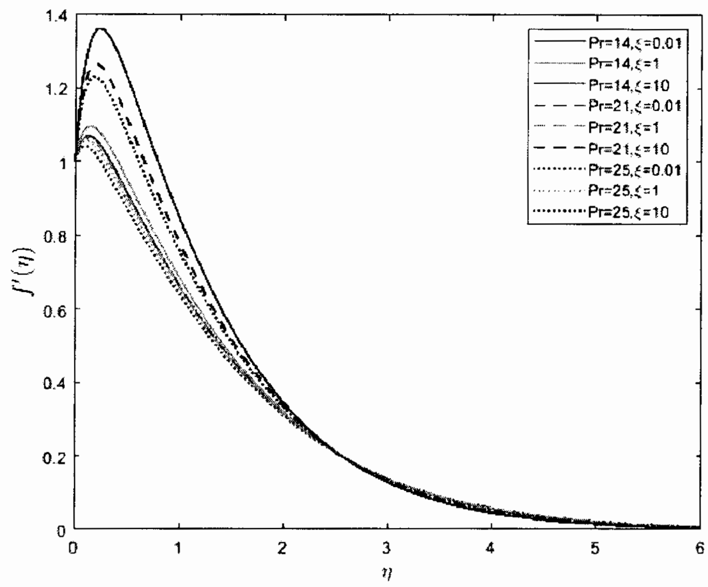

Fig. 5. $f'(\eta)$ versus η for different Pr and ξ.

Figures 6–9 represent the consequences of various B, N, θ_r and Pr along with different ξ on the temperature distribution respectively for the same fixed values mentioned earlier. It is evident from all four of the figures that the temperature profiles diminish with elevating buoyancy force parameter ξ, although Free convection currents are aided, and thus heat is transported more efficiently.

Also note that, considering a fixed ξ, as the values of B, N, and Pr increase, the temperature profiles decrease but they get increased with increasing $|\theta_r|$. That

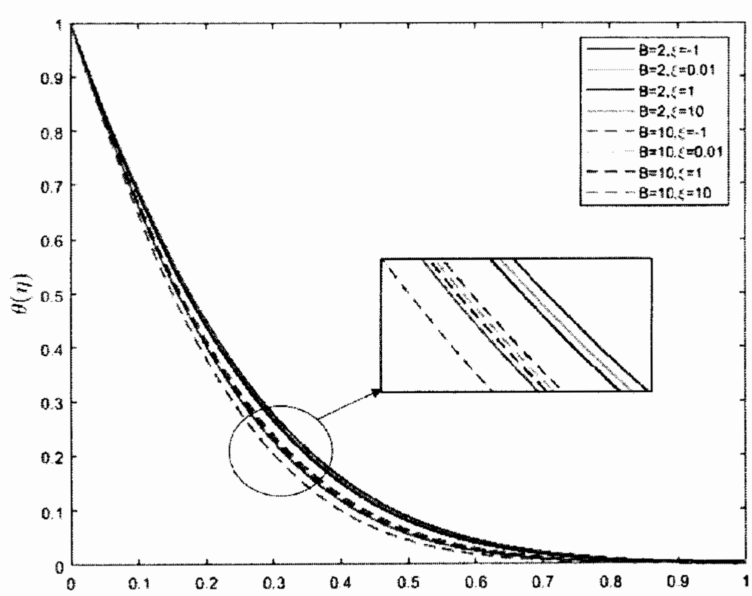

Fig. 6. $\theta(\eta)$ versus η for different B and ξ.

subito e.V. licensed customer copy supplied for Library and Information Service (SLI02X00670E)

J. Mech. Med. Biol. Downloaded from www.worldscientific.com
by SWISS FEDERAL INSTITUTE OF TECHNOLOGY ZURICH (ETH) on 09/26/22. Re-use and distribution is strictly not permitted, except for Open Access articles.

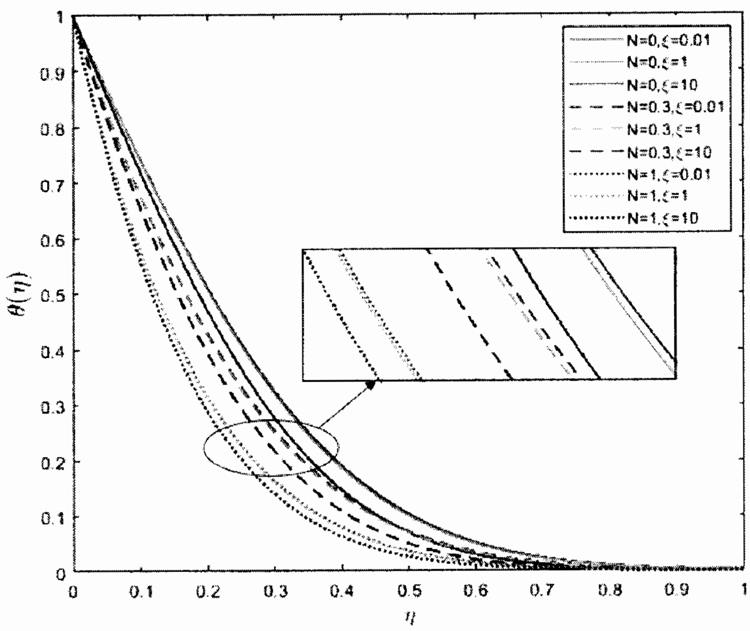

Fig. 7. $\theta(\eta)$ versus η for different N and ξ.

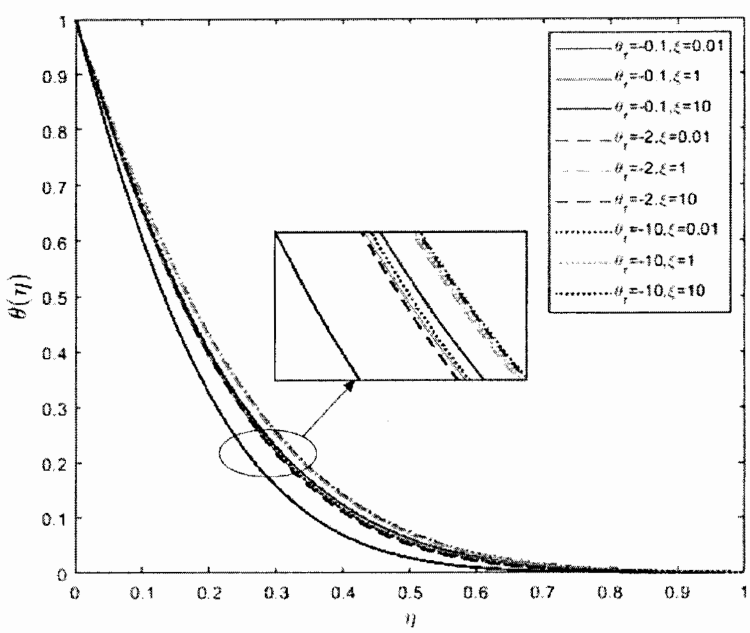

Fig. 8. $\theta(\eta)$ versus η for different θ_r and ξ.

means, the thermal boundary-layer thickness gets shrunk with higher values of B, N, and Pr but it expands with higher θ_r. Note that the variation in temperature profiles are prominent within the region $(0.2 \leq \eta \leq 0.6)$ due to the impact of B and θ_r along with ξ. Whereas, the effect of the parameters N and Pr are prominent within $(0.1 \leq \eta \leq 0.6)$ and thereafter the curves asymptotically decay to zero. Also note

subito e.V. licensed customer copy supplied for Library and Information Service (SLI02X00670E)

J. Mech. Med. Biol. Downloaded from www.worldscientific.com by SWISS FEDERAL INSTITUTE OF TECHNOLOGY ZURICH (ETH) on 09/26/22. Re-use and distribution is strictly not permitted, except for Open Access articles.

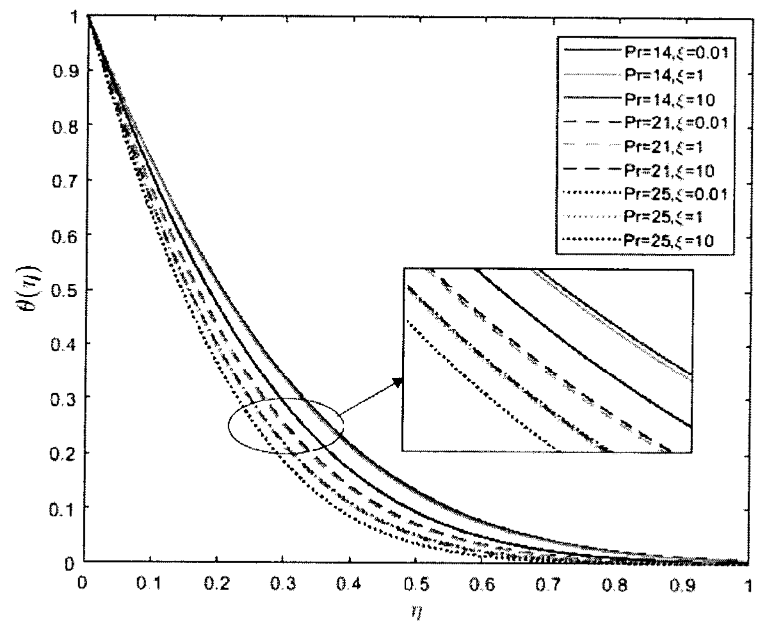

Fig. 9. $\theta(\eta)$ versus η for different Pr and ξ.

that, unlike the velocity distribution, the enhancement in temperature profile is sustained throughout the entire region.

Figure 10 demonstrates the variation of skin friction coefficient and heat transfer rate as a function of ξ with different values of B, taking $\Pr = 21$, $N = 0.3$, $\theta_r = -2.0$. It is observed that both skin friction coefficient and heat transfer rate are increasing functions of ξ for any fixed B. As ξ is increasing, higher values of B result in higher values of the friction factor as well as heat transfer rate. These physically mean that as the effect of the magnetic field becomes comperatively

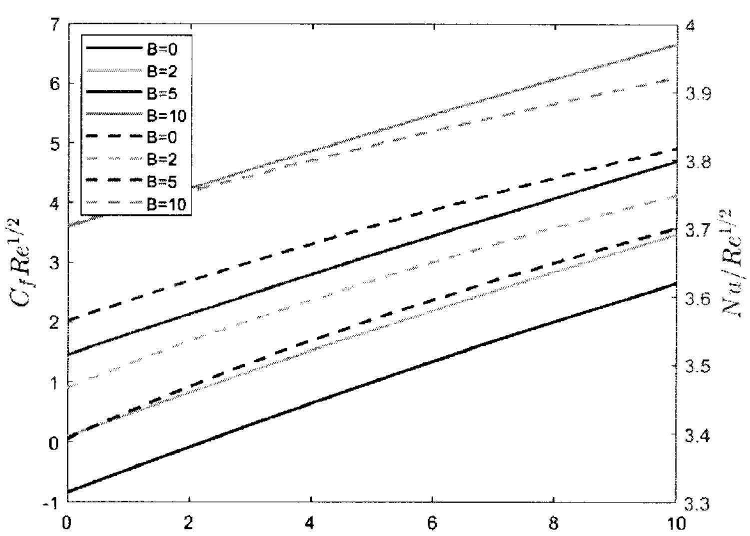

Fig. 10. Effects of B on $C_f\mathrm{Re}^{1/2}$ and $\mathrm{Nu}/\mathrm{Re}^{1/2}$ as a function of ξ.

subito e.V. licensed customer copy supplied for Library and Information Service (SLI02X00670E)

J. Mech. Med. Biol. Downloaded from www.worldscientific.com
by SWISS FEDERAL INSTITUTE OF TECHNOLOGY ZURICH (ETH) on 09/26/22. Re-use and distribution is strictly not permitted, except for Open Access articles.

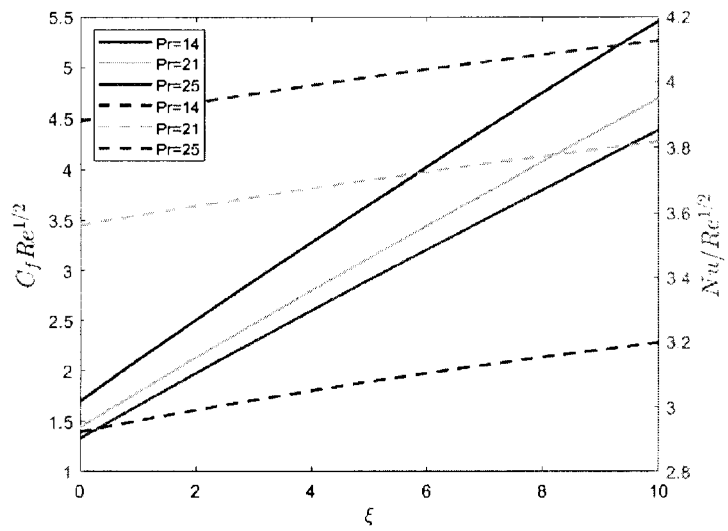

Fig. 11. Effects of Pr on $C_f\mathrm{Re}^{1/2}$ and $\mathrm{Nu}/\mathrm{Re}^{1/2}$ as a function of ξ.

significant, shearing stress exerted by the fluid at the sheet as well as the rate of heat transfer get higher.

The results of the skin friction coefficient and heat transfer rate (Nusselt number) are indicated in Fig. 11 against ξ for selected values of Pr, taking $B = 5$, $N = 0.3$, $\theta_r = -2.0$. We notice that as ξ is increasing, larger values of the Pr brings about lower values in the skin friction coefficient yet higher values in heat transfer rate. This phenomenon explains that fluids with higher Prandtl number experience lower shearing stress but possess higher heat capacity and thus, the enhancement in rate of heat transfer. The trend of the skin friction coefficient and heat transfer rate graphs are both rising with increasing values of ξ and any fixed Pr.

The impacts of N and θ_r along with ξ on the skin friction coefficient and heat transfer rate are illustrated at Figs. 12 and 13. It is observed that as ξ is increasing,

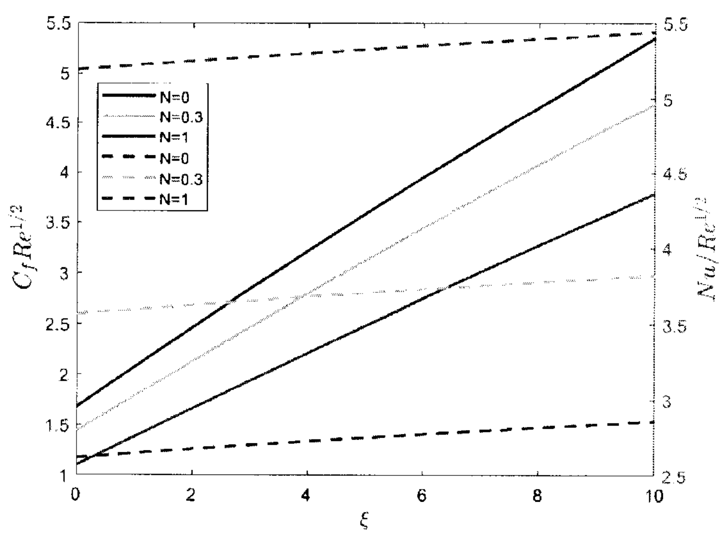

Fig. 12. Effects of N on $C_f\mathrm{Re}^{1/2}$ and $\mathrm{Nu}/\mathrm{Re}^{1/2}$ as a function of ξ.

subito e.V. licensed customer copy supplied for Library and Information Service (SLI02X00670E)

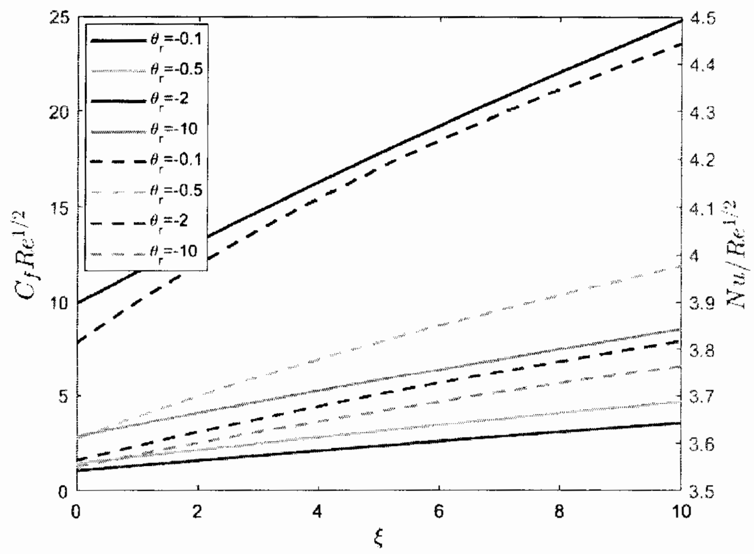

Fig. 13. Effects of θ_r on $C_f\mathrm{Re}^{1/2}$ and $\mathrm{Nu}/\mathrm{Re}^{1/2}$ as a function of ξ.

higher values of N result in lower values of the friction factor but higher values in heat transfer rate. Whereas, the skin friction and Nusselt number, respectively, elevates and reduces with increasing $|\theta_r|$. Note that the effect of lower value of $|\theta_r|$ is more significant in both stress factor and heat transfer rate as we can notice that $\theta_r = -0.1$ gives the highest Nusselt number distribution and lowest friction factor distribution.

Figures 14–19 indicate the distributions of skin friction coefficient and heat transfer rate as a function of B with the combination of different Pr, N, θ_r and ξ. In general, it is evident from all these figures that, both $C_f\mathrm{Re}^{1/2}$ and $\mathrm{Nu}/\mathrm{Re}^{1/2}$ are

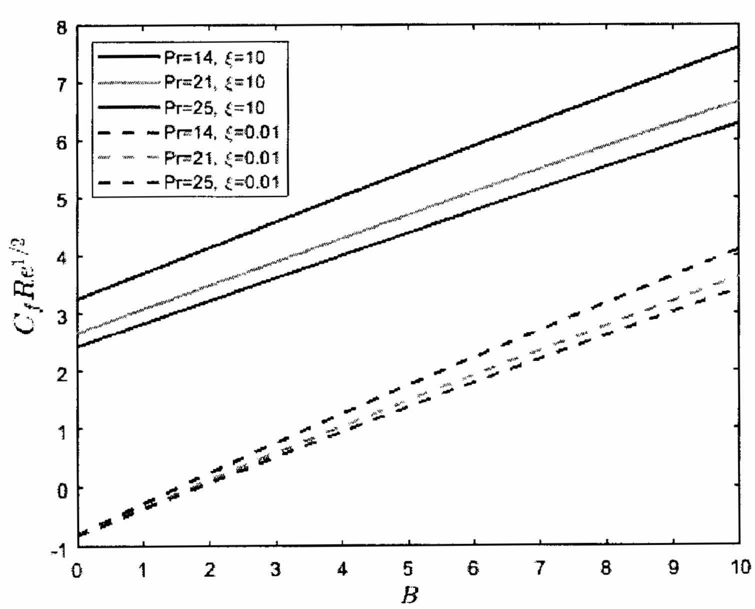

Fig. 14. $C_f\mathrm{Re}^{1/2}$ versus B for different values of Pr and ξ.

J. Mech. Med. Biol. Downloaded from www.worldscientific.com by SWISS FEDERAL INSTITUTE OF TECHNOLOGY ZURICH (ETH) on 09/26/22. Re-use and distribution is strictly not permitted, except for Open Access articles.

subito e.V. licensed customer copy supplied for Library and Information Service (SLI02X00670E)

J. Mech. Med. Biol. Downloaded from www.worldscientific.com
by SWISS FEDERAL INSTITUTE OF TECHNOLOGY ZURICH (ETH) on 09/26/22. Re-use and distribution is strictly not permitted, except for Open Access articles.

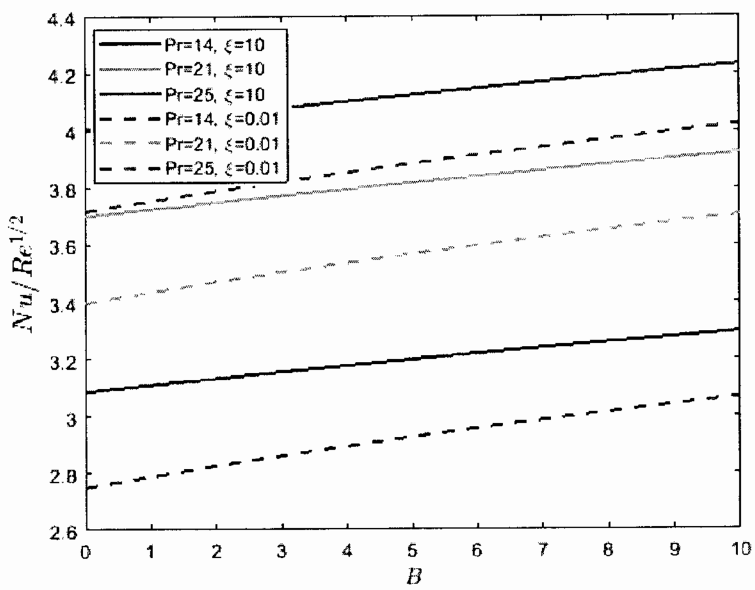

Fig. 15. $\mathrm{Nu}/\mathrm{Re}^{1/2}$ versus B for different values of Pr and ξ.

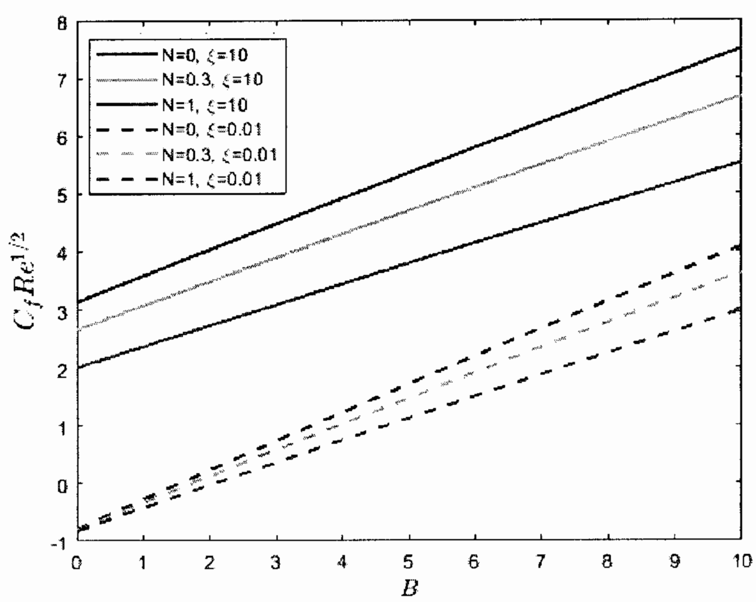

Fig. 16. $C_f\mathrm{Re}^{1/2}$ versus B for different values of N and ξ.

increasing with the B. Moreover, all the figures exhibit higher values in the free convection case ($\xi \gg 1$) than the forced convection case ($\xi \ll 1$). The impact of Pr and N on the friction factor are quite similar in the sense that both of these parameters have an inverse effect on the growth of the skin friction coefficient distributions. But note that these parameters have a linearly proportional effect on Nusselt number.

We have observed quite interesting outcomes in the skin friction coefficient and heat transfer rate distribution for varying B and θ_r, as shown in Figs. 18 and 19. For

subito e.V. licensed customer copy supplied for Library and Information Service (SLI02X00670E)

J. Mech. Med. Biol. Downloaded from www.worldscientific.com
by SWISS FEDERAL INSTITUTE OF TECHNOLOGY ZURICH (ETH) on 09/26/22. Re-use and distribution is strictly not permitted, except for Open Access articles.

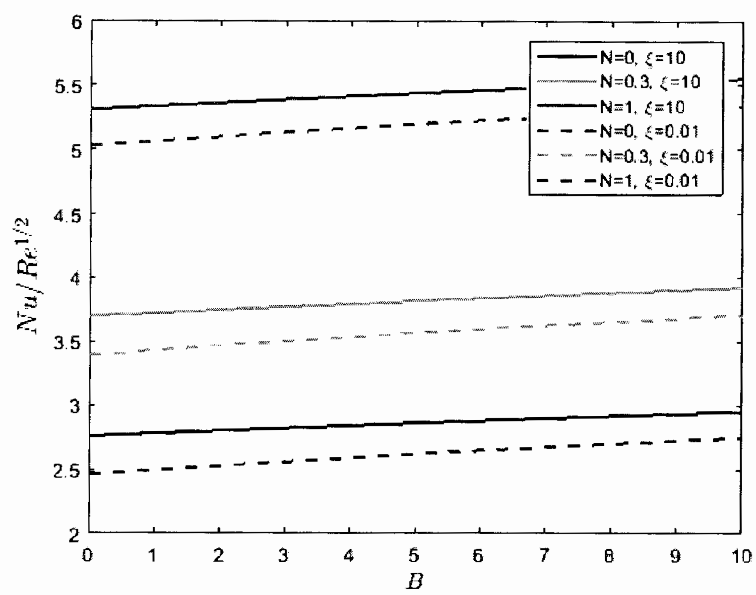

Fig. 17. $\mathrm{Nu}/\mathrm{Re}^{1/2}$ versus B for different values of N and ξ.

the free convection case, as B increases, the friction factor increases with increasing $|\theta_r|$ continuously. In the forced convection case, we observe that initially $C_f\mathrm{Re}^{1/2}$ decreases with increasing $|\theta_r|$ up to the point $B \sim 4$, and after the point $B \sim 5$, the skin friction coefficient increases with $|\theta_r|$. The opposite case is noticed in heat transfer rate distributions. As B increases, the rate of heat transfer reduces continuously with increasing $|\theta_r|$, in the forced convection case. But $\mathrm{Nu}/\mathrm{Re}^{1/2}$ initially escalates with $|\theta_r|$ up to $B \sim 2$ and beyond that point, it starts decreasing with $|\theta_r|$.

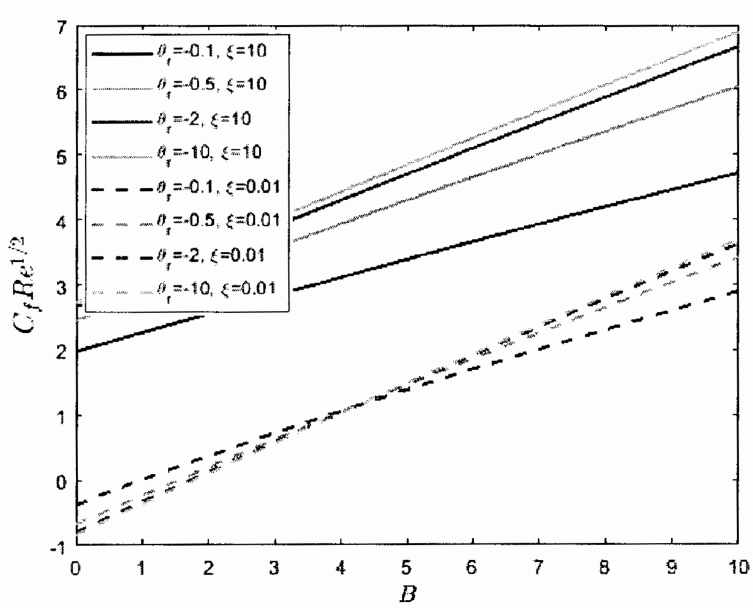

Fig. 18. $C_f\mathrm{Re}^{1/2}$ versus B for different values of θ_r and ξ.

subito e.V. licensed customer copy supplied for Library and Information Service (SLI02X00670E)

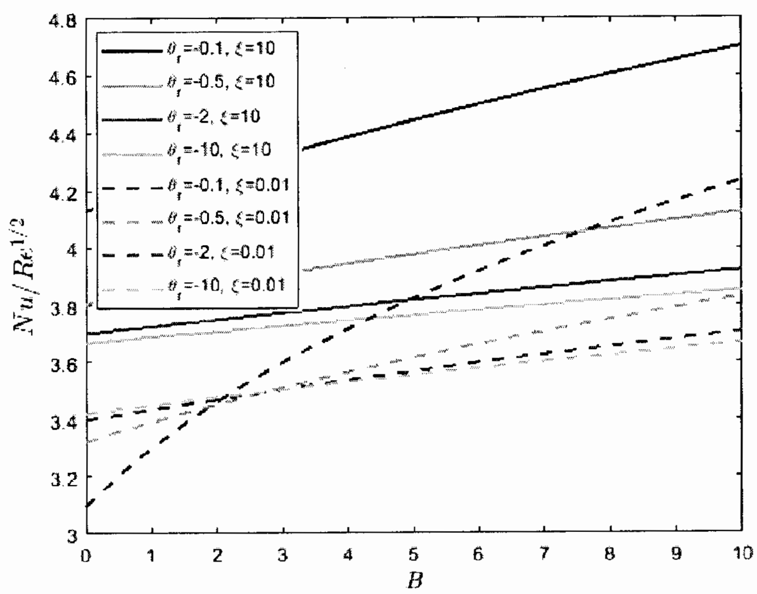

Fig. 19. $\mathrm{Nu}/\mathrm{Re}^{1/2}$ versus B for different values of θ_r and ξ.

5. Conclusion

In this study, the steady, 2D, laminar mixed convective boundary-layer flow of a Newtonian viscous incompressible biological fluid (blood) embedded by a magnetic dipole is analysed. The flow is considered along a continuously moving horizontal sheet. Imposing appropriate similarity transformations, the dimensionless ordinary differential boundary value problem has been solved numerically using a stable, accurate finite difference method. Verification with former researches for selected cases of the general model has been conducted. The influences of various governing factors (i.e., buoyancy force parameter, ferromagnetic interaction intensity, Prandtl number, variable wall parameter, viscosity-temperature parameter) on the flow profiles as well as on the skin friction coefficient, and the heat transfer rate are scrutinized meticulously. The vital assessments of the current work are encapsulated as follows:

- The flow is accelerated with higher buoyancy force parameter and ferromagnetic interaction parameter but decelerated with the increment of variable wall parameter, viscosity-temperature parameter and Prandtl number.
- Temperture diminishes with higher values of buoyancy force parameter, ferromagnetic interaction parameter, variable wall parameter and Prandtl number but gets elevated with the increasing value of viscosity-temperature parameter.
- Although the distribution of temperature due to the impact of the parameters is persistent all over the entire region, the velocity profiles gets separated at certain points and hence reversed.

subito e.V. licensed customer copy supplied for Library and Information Service (SLI02X00670E)

J. Mech. Med. Biol. Downloaded from www.worldscientific.com by SWISS FEDERAL INSTITUTE OF TECHNOLOGY ZURICH (ETH) on 09/26/22. Re-use and distribution is strictly not permitted, except for Open Access articles.

J. Mech. Med. Biol. Downloaded from www.worldscientific.com by SWISS FEDERAL INSTITUTE OF TECHNOLOGY ZURICH (ETH) on 09/26/22. Re-use and distribution is strictly not permitted, except for Open Access articles.

- Skin friction factor is found to elevate with greater buoyancy force parameter, ferromagnetic interaction parameter and viscosity-temperature parameter, whereas it gets suppressed with larger Prandtl number and variable wall parameter.
- Except for the viscosity-temperature parameter, all the other parameters have an increasing effect on the heat transfer rate (Nusselt number).

Acknowledgments

We have presented this work in "ICHMT International Symposium on Advances in Computational Heat Transfer" occurred in Rio de Janeiro, Brazil on August 15–19, 2021.

References

1. Abi-Abdallah D, Drochon A, Robin V, Fokapu O, Effects of static magnetic field exposure on blood flow, *Eur Phys J* **45**(1):451–467, 2009.
2. Abi-Abdallah D, Drochon A, Robin V, Fokapu O, Pulsed magnetohydrodynamics blood flow in a rigid vessel under physiological pressure gradient, *Comput Methods Biomech Biomed Eng* **12**:445–458, 2009.
3. Gul A, Tzirtzilakis EE, Makhanov SS, Simulation of targeted magnetic drug delivery: Two-way coupled biomagnetic fluid dynamics approach, *Phys Fluids* **34**:021911, 2022.
4. Alam J, Murtaza G, Tzirtzilakis E, Ferdows M, Biomagnetic fluid flow and heat transfer study of blood with gold nanoparticles over a stretching sheet in the presence of magnetic dipole, *Fluids* **6**:113, 2021.
5. Ali M, Al-Yousef F, Laminar mixed convection from a continuously moving vertical surface with suction or injection, *Heat and Mass Transfer* **33**(4):301–306, 1998.
6. Ali ME, The effect of variable viscosity on mixed convection heat transfer along a vertical moving surface, *Int J Therm Sci* **45**(1):60–69, 2006.
7. Andersson HI, Valnes OA, Flow of a heated ferrofluid over a stretching sheet in the presence of a magnetic dipole, *Acta Mech* **128**:39–47, 1998.
8. Sharifi A, Motlagh SY, Badfar H, Ferro hydro dynamic analysis of heat transfer and biomagnetic fluid flow in channel under the effect of two inclined permanent magnets, *J Magnet Magetic Mater* **472**:115–122, 2019.
9. Ayeche CM, Kezzar M, Sari MR, Eid MR, Analytical ADM study of time-dependent hydromagnetic flow of biofluid over a wedge, *Indian J Phys* **95**(12):2769–2784, 2021.
10. Bachok N, Ishak A, Pop I, Mixed convection boundary layer flow over a moving vertical flat plate in an external fluid flow with viscous dissipation effect, *Plos One* **8**:4, 2013.
11. Beg OA, Beg TA, Kadir A, Leonard HJ, Malysheva LI, Khan UF, El Gendy M, Numerical simulation of biomagnetic micropolar blood flow with the Rosensweig ferromagnetic formulation, *ICFMA 2022: 16th Int. Conf. Fluid Mechanics and Applications*, 28th–29th October 2022, Lisbon, Portugal, 2020.
12. Chato JC, Heat transfer to blood vessels, *J Biomech Eng* **102**:110–118, 1980.
13. Crane LJ, Flow past a stretching plate, *Z Angew Math Phys* **21**(4):645–647, 1970.
14. Cramer KR, Pai SI, *Magnetofluid Dynamics for Engineers and Applied Physicists*, Scripta Publishing Company, Washington DC, 1973.
15. Davidson PA, *An Introduction to Magnetohydrodynamics*, Cambridge University Press, Cambridge, 2001.

subito e.V. licensed customer copy supplied for Library and Information Service (SLI02X00670E)

J. Mech. Med. Biol. Downloaded from www.worldscientific.com
by SWISS FEDERAL INSTITUTE OF TECHNOLOGY ZURICH (ETH) on 09/26/22. Re-use and distribution is strictly not permitted, except for Open Access articles.

16. Dholey S, Effect of magnetic field on the unsteady boundary layer flows induced by an impulsive motion of a plane surface, *Z Naturforsch* **75**(4):343–355, 2020.
17. Ferdows M, Alam J, Murtaza G, Tzirtzilakis EE, Sun S, Biomagnetic flow with $CoFe_2O_4$ magnetic particles through an unsteady stretching/shrinking cylinder, *Magnetochemistry* **8**, 27, 2022.
18. Haik Y, Paiand V, Chen J, Development of magnetic device for cell separation, *J Magnet Magnet Mater* **194**(1–3):254–261, 1999.
19. Hassanien IA, The effects of variable viscosity on flow and heat transfer on a continuous stretching surface, *ZAMM* **77**(11):876–880, 1997.
20. Hughes WF, Young FJ, *The Electromagnetodynamics of Fluids*, 1st edn (John Wiley & Sons, New York, 1966).
21. Alam J, Murtaza MG, Tzirtzilakis EE, Ferdows M, Magnetohydrodynamic and ferrohydrodynamic interactions on the biomagnetic flow and heat transfer containing magnetic particles along a stretched cylinder, *Eur J Comput Mech* **31**(1):1–40, 2022.
22. Kafoussias NG, Raptis A, Tzirtzilakis EE, Free-forced convective boundary layer flow of a biomagnetic fluid flow under the action of a localized magnetic field, *Canad J Phys* **86**(3):447–457, 2008.
23. Karwe MV, Jaluria Y, Fluid flow and mixed convection transport from a moving plate in rolling and extrusion processes, *J Heat Transfer* **110**(3):655–661, 1988.
24. Karwe MV, Jaluria Y, Numerical simulation of thermal transport associated with a continuously moving flat sheet in materials processing, *J Heat Transfer* **113**(3):612–619, 1991.
25. Ling JX, Dybbs A, Forced convection over a flat plate submerged in a porous medium, *Paper 87-WA/HT-23* (ASME, New York, 1987).
26. Mamun K, Funazaki K, Akter S, Akhter MN, The effect of magnetic field on blood flow through stenotic artery: A review on bio-magnetic fluid dynamics, *Ser Biomech* **34**(1):20–30, 2020.
27. Mckay JC, Prato FS, Thomas AW, A literature review: The effects of magnetic field exposure on blood flow and blood vessels in the microvasculature, *Bioelectromagnetics* **28**:81–98, 2007.
28. Misra JC, Shit GC, Biomagnetic viscoelastic fluid flow over a stretching sheet, *Appl Mathemat Comput* **210**(2):350–361, 2009.
29. Ferdows M, Alzahrani F, Sun S, Dual solution of boundary-layer flow driven by variable plate and streaming-free velocity, *Adv Mech Eng* **12**(7):1–7, 2020.
30. Murtaza MG, Tzirtzilakis EE, Ferdows M, Effect of electrical conductivity and magnetization on the biomagnetic fluid flow over a stretching sheet, *Z Angew Math Phys* **68**(93):1–15, 2017.
31. Murtaza MG, Tzirtzilakis EE, Ferdows M, Similarity solutions of nonlinear stretched biomagnetic flow and heat transfer with signum function and temperature power law geometries, *Int J Mathemat Comput Sci* **12**(2):9–14, 2018.
32. Murtaza MG, Tzirtzilakis EE, Ferdows M, A Duality of biomagnetic fluid flow and heat transfer over a quadratic stretched sheet, *J Power Technol* **101**(3):154–162, 2021.
33. Mousavi SM, Darzi AA, Akbari OA, Toghraie D, Marzban A, Numerical study of biomagnetic fluid flow in a duct with a constriction affected by a magnetic field, *J Magnet Magnet Mater* **473**(3):42–50, 2019.
34. Murtaza MG, Tzirtzilakis EE, Ferdows M, Stability and convergence analysis of a biomagnetic fluid flow over a stretching sheetin the presence of a magnetic field, *Symmetry* **12**:253, 2020, doi: 10.3390/sym12020253, 2020.
35. Najib N, Bachok N, Md Arifin N, Pop I, Dual solutions on boundary layer flow over a moving surface in a flowing nanofluid with second order slip, *Thermal Sci* **24**(2):1117–1129, 2020.

subito e.V. licensed customer copy supplied for Library and Information Service (SLI02X00670E)

J. Mech. Med. Biol. Downloaded from www.worldscientific.com
by SWISS FEDERAL INSTITUTE OF TECHNOLOGY ZURICH (ETH) on 09/26/22. Re-use and distribution is strictly not permitted, except for Open Access articles.

36. Neuringer JL, Rosensweig RE, Ferrohydrodynamics, *Phys Fluids* **7**:1927, 1964.
37. Amirah Idris N, Amin N, Rahmat H, Effect of gravitational acceleration on unsteady bio-magnetic fluid flow, *Appl Comput Mathemat* **3**(6):285–294, 2014.
38. Pop I, Gorla RSR, Rashidi M, The effect of variable viscosity on flow and heat transfer to a continuous moving flat plate, *Int J Eng Sci* **30**(1):1–5, 1992.
39. Titus R, Abraham A, Ferromagnetic liquid flow due to gravity-Aligned stretching of an elastic sheet, *J Appl Fluid Mech* **8**(3):591–600, 2015.
40. Ravindran R, Samyuktha N, Unsteady mixed convection flow over a stretching sheet in presence of chemical reaction and heat generation or absorption with no-uniform slot suction or injection, *Appl Mathemat Mech* **36**:1253–1272, 2015.
41. Rosensweig RE, *Ferrohydrodynamics*, Cambridge University Press, Cambridge, 1985.
42. Rosensweig RE, Magnetic fluids, *Ann Rev Fluid Mech* **19**:437–463, 1987.
43. Sakiadis BC, Boundary layer behaviour on continuous solid surface: I. Boundary-layer equations for two dimensional and axisymmetric flow, *AICHE J* **7**(1):26–28, 1961.
44. Sakiadis BC, Boundary layer behaviour on continuous solid surface: II. Boundary-layer on a continous flat surface, *AICHE J* **1**:221–225, 1961.
45. Sankar DS, Lee U, FDH analysis for MHD flow of a non-Newtonian fluid for blood flow in stenosis, *J Mech Sci Technol* **25**:2573–2581, 2011.
46. Singh P, Kumar M, Free convection in heat transfer flow over a moving sheet in Aluminia water nanofluid, *J Eng*, **2014**:137426, 2014, doi: 10.1155/2014/137426.
47. Soundalgekar VM, Takhar HS, Das UN, Deka RK, Sarmah A, Effect of variable viscosity on boundary layer flow along a continuously moving plate with variable surface temperature, *Heat Mass Transfer* **40**:421–424, 2004.
48. Sutton GW, Sherman A, *Engineering Magnetohydrodynamics*, McGraw-Hill, New York, 1965.
49. Tzirtzilakis EE, Kafoussias NG, Bio-magnetic fluid flow over a stretching sheet with nonlinear temperature dependent magnetization, *Z Angew Math Phys* **54**:551–565, 2003.
50. Tzirtzilakis EE, A mathematical model for blood flow in magnetic field, *Physics Fluids* **17**(7):077103–077115, 2005.
51. Tzirtzilakis EE, Biomagnetic fluid flow in a channel with stenosis, *Physica D* **237**:66–81, 2008.

subito e.V. licensed customer copy supplied for Library and Information Service (SLI02X00670E)